Thin films of Co on Pt(111): Strain relaxation and growth

E. Lundgren, B. Stanka, M. Schmid, and P. Varga
Institut für Allgemeine Physik, TU Wien, Wiedner Hauptstrasse 8-10, A-1040, Austria
(Received 10 November 1999; revised manuscript received 8 February 2000)

The growth, structure and morphology of thin Co layers with a thickness ranging from 1 to 15 monolayers deposited at room temperature on Pt(111) have been studied by the use of scanning tunneling microscopy. We demonstrate that the first Co layer grows preferably in the Pt fcc lattice sites, with a high density of defects due to the lattice mismatch. The second Co layer is found to exhibit a moiré structure, with the Co in-plane lattice distance close to that of bulk Co. The growth of thin Co films is observed to be mostly in terms of flat layers (two dimensional) up to a Co coverage of about 3.5 ML. At higher coverages, we find that the Co grows in (three dimensional) islands and we show that the growth is characterized by a mainly twinned fcc-like stacking. We argue that the reason for the two dimensional growth mode at lower Co coverages is due to the strained interface between the Co overlayers and the Pt(111) surface resulting in a large number of kinks and corners which facilitate interlayer diffusion. For higher coverage such sites become less common, due to the decreasing influence of the strained interface, resulting in no interlayer diffusion leading to a three dimensional growth mode. The implications by these observations on the magnetic properties of the Co/Pt(111) interface system are discussed.

I. INTRODUCTION

The structure of heteroepitaxial thin metal films on metal substrates has been studied for many years.[1] This large interest has been driven by the desire to link the geometrical structure of the interface between the thin film and the substrate with magnetic and/or electronic properties observed at the interface. In the case of Co-Pt thin films and multilayer systems, particular magnetic properties such as the perpendicular magnetic anisotropy (PMA) have been observed for very thin Co layers in Co-Pt multilayers.[2–4] The direction of the magnetic anisotropy has been found to depend on the details of the geometric structure at the interface. For instance, the thickness of the Co layers has been found to influence the PMA,[5,6] which has been related to a fcc-to-hcp transition in the Co layers as the Co thickness is increased. Due to the complexity of a multilayer interface system, it is fruitful to study and gain understanding of the magnetic and geometric properties during the initial interface formation for a single Co and Pt interface, such as the Co/Pt(111) interface.

A recent surface magnetooptical Kerr effect (SMOKE) study of thin Co films on Pt(111) (Ref. 7) reports a linear increase of the PMA as the Co coverage is increased from 0.8 to 3.7 ML [1 ML is defined here as the amount of atoms in one Pt(111) layer]. At a Co coverage between 4 and 6 ML, in-plane and out-of-plane magnetization was found to coexist. The out-of-plane magnetization was observed to decrease to zero at about 6 ML of Co, whereas the in-plane magnetization continued to increase. Such a behavior, which is also similar to that of Co-Pt multilayers, merits a detailed structural investigation.

In fact, the structure and morphology of thin Co deposits on Pt(111) has been studied extensively in the past.[8–15]

For instance, Grütter and Dürig have previously used scanning tunneling microscopy (STM) in order to study thin Co films deposited on Pt(111) (Ref. 8) at room temperature (RT). They reported a quasi–layer-by-layer growth mode up to a Co coverage of 3 ML, including a large number of defects in the first layer and a moiré structure in the second layer. Above 3 ML a three-dimensional (3D) growth mode was observed and furthermore it was shown that Co grows in a hcp stacking sequence above 3 ML. At higher Co coverages the Co film appeared granular. Co growing in a predominantly hcp stacking was also found by an extended x-ray absorption fine structure (EXAFS) study for Co films thicker than 4 ML.[10]

Low-energy-electron-diffraction studies (LEED)[4,11–13] have shown that the first ML is nearly epitaxial on the Pt(111) surface, since no extra spots where observed in this coverage regime. Above approximately 1.5 ML of Co, additional LEED spots become visible, corresponding to that of the in-plane lattice constant of bulk Co (9.4% smaller than that of Pt), implying that the Co lattice, at this Co coverage, relaxes to close to that of bulk Co. At higher Co coverages a sixfold fine structure appears around each spot, interpreted as a modulation of the Co overlayer, consistent with the STM observations of the moiré structure[8] due to a large coincidence cell of the modulated surface structure.

Surface x-ray-diffraction (SXRD) experiments[14] concluded that a multilevel surface consisting of five different levels is formed after Co deposition of 3 ML. The most dominant feature observed up to a Co coverage of six layers was a component in the out-of-plane diffraction due to disorder in the lattice constant in the out-of-plane direction, again consistent with the modulated surface structure of a moiré structure. At higher coverages, 8 and 12 ML, the stacking of the Co was found to be predominantly twinned fcc. For a 10 ML thick Co film deposited at RT, a Co film consisting of planes stacked in fcc, twinned fcc and hcp has also been reported.[15]

In this paper we present STM results from Co thin films deposited on Pt(111) at RT. We show that the Co atoms in the first Co layer take preferably the Pt fcc lattice sites; the

induced tensile strain in the Co layer is relieved by partial dislocations (surface defects). The second Co layer, which is observed to relieve the partial dislocations, displays a moiré structure; the Co in-plane lattice parameter is found to take a value close to that of bulk Co. The moiré structure is found to persist up to a coverage of at least 5 ML. The growth of the Co film is observed to be almost flat or two dimensional (2D) up to a Co coverage of about 3.5 ML. At coverages of 5 ML and higher, islands exhibiting a three-dimensional (3D) growth are observed. These islands are found to grow in a predominantly twinned fcc-like stacking. Finally, the present structural findings are discussed in relation to previous findings of the magnetic properties of the Co/Pt(111) interface.

II. EXPERIMENT

The STM and AES measurements were performed in a UHV chamber with a base pressure below 5×10^{-11} mbar. All STM images were obtained in constant current mode with the sample negative. The Pt sample was prepared in a separate chamber with a base pressure of approximately 1×10^{-10} mbar. The sample was cleaned by cycles of 2 keV Ar^+ sputtering followed by annealing at 1150 K. The cleanliness of the Pt(111) surface and of the Co prepared surfaces was checked by AES; no contaminants such as C and O could be observed within the detection limits. The clean Pt(111) surface exhibited a distinctive (1×1) LEED pattern. The size of the terraces of the sample was found to be 10–50 nm as observed with STM. Co was deposited from a water-cooled electron beam evaporator. The typical evaporation rate was 1 ML/2 min as measured by a quartz crystal microbalance. In separate experiments, to avoid adsorption of residual gas, the sample was kept at 600 K until shortly before the Co evaporation, and the evaporator was cooled with liquid nitrogen, resulting in a pressure well below 1×10^{-10} mbar during evaporation. No difference was found in the results from these preparations. A retarding voltage was applied to the end of the evaporator in order to suppress Co ions from the evaporator, since such ions have previously been found to influence the growth of thin films.[16] The error in Co coverage was estimated from repeated measurements to be less than 10% as determined from the ratio between the Co 773 eV and the Pt 237 eV Auger peak-to-peak signals.

III. RESULTS

This section is separated into two subsections. In the first subsection, we present results from low coverages of Co on the Pt(111) surface mainly focusing on misfit phenomena. In the second subsection, the results from high Co coverages are presented, and the stacking sequence of the Co adislands will be discussed.

A. Low Co coverages on the Pt(111) surface (1–5 ML)

Figure 1 shows an STM image from a 1.2 ML thick Co film deposited on Pt(111) at RT. From the image, three different areas may be observed: (a) the Pt (111) surface, (b) the first Co layer directly on top of the Pt(111) surface layer, and (c) the second Co layer on top of the first Co layer. The different areas are indicated in Fig. 1.

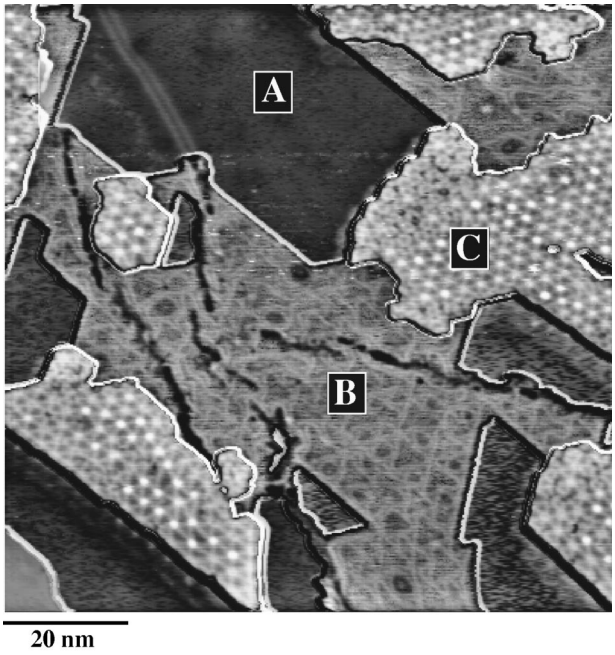

FIG. 1. STM image of a Pt(111) surface with a 1.2 ML thick Co film deposited at RT displaying three different levels: (a) Uncovered part of the Pt(111) surface, (b) the first Co layer, (c) the second Co layer. The image has been enhanced in order to display the three levels simultaneously, leading to artefacts at the steps. The noise observed in the lower part of the image is due to an unstable tip.

STM images with higher resolution from the corresponding areas as shown in Fig. 1 are presented in Fig. 2. It should be noted that the images shown in Fig. 2 are not recorded from the same preparation as in Fig. 1, but are selected images from different preparations in order to highlight the features observed in Fig. 1. Figure 2(a) shows an STM image with chemical contrast from the Pt(111) surface which is not covered by Co, corresponding to region A in Fig. 1. The image displays a Co-induced double line reconstruction of the Pt(111) surface due to tensile strain in the Pt surface; the darker atoms on the left-hand side of the image are Co atoms incorporated into the Pt(111) surface. The Co-induced double line reconstruction and dendrite formation on Pt(111) has been discussed in detail elsewhere.[9,17] The present results show that the Co-induced double line reconstruction may be formed at a temperature as low as RT, however the number of the double lines at this temperature is lower than at temperatures slightly above RT.

Turning to the appearance of the first Co layer, Fig. 2(b) shows an STM image with chemical contrast of Co on Pt(111) from a 1.2 ML thick Co film deposited on Pt(111) at RT, corresponding to region B in Fig. 1. The image shows Co atoms which have diffused and attached to a Pt step edge (lower right part of the image), thus the atoms underneath the Co atoms are Pt atoms. The bright spot in the image (upper left) is due to second-layer Co atoms adsorbed on the first Co layer. In the first Co layer, lines of brighter Co atoms may be observed. A line drawn in the $[1\bar{1}0]$ direction across such bright lines, as indicated in the close-up STM image in Fig. 3(a), demonstrates that the Co atoms in this direction are not in a straight row. The direction of the shift of the atoms in between the brighter lines results in the sketch in Fig. 3(b), in

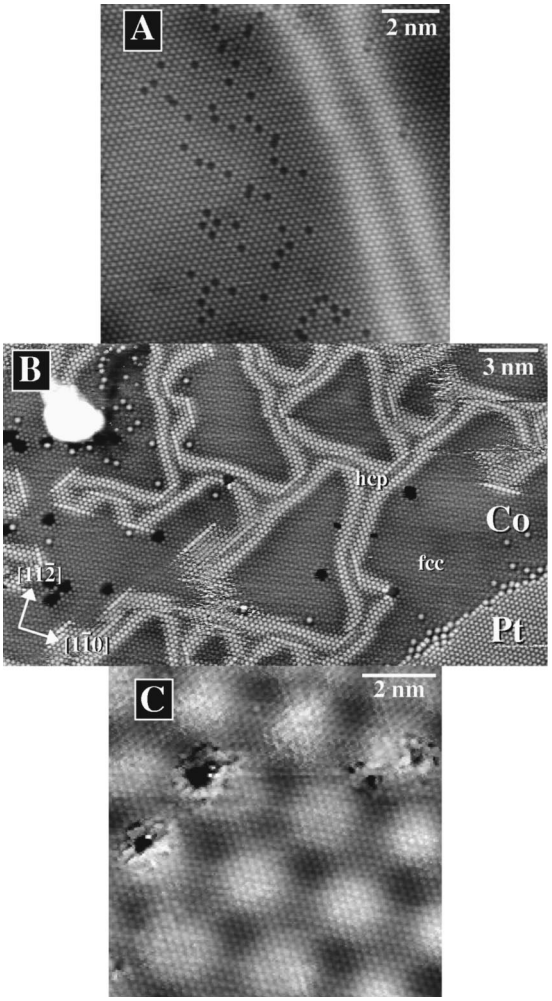

FIG. 2. STM images from areas corresponding to those shown in Fig. 1, but with higher resolution. (a) STM image with chemical contrast of the uncovered Pt(111) surface, displaying a Co induced double line reconstruction (Refs. 9 and 17) and single Co atoms embedded in the first Pt layer. (b) STM image with chemical contrast of the first Co layer, displaying a dislocation network. (c) STM image with atomic resolution of the second Co layer, displaying a moiré structure.

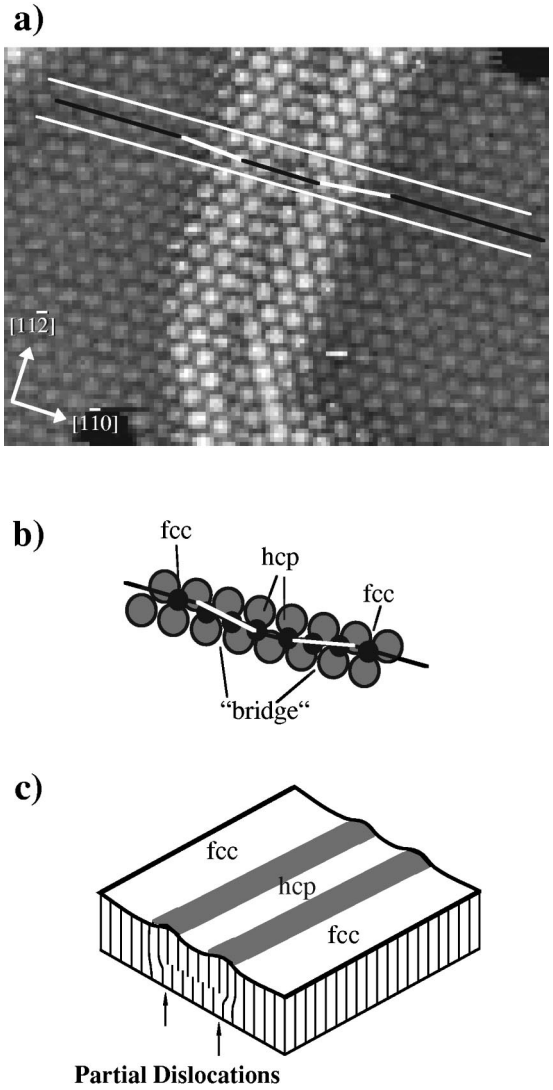

FIG. 3. Model for the features observed in Fig. 2(b). (a) Close-up of the STM image in Fig. 2(b). The lines drawn demonstrates that the Co atoms are not in a straight line across the stacking fault region. (b) Top view of a model of the stacking fault region, the black topmost spheres being Co atoms. Based on the known crystallographic directions of the substrate, it can be determined that the Co atoms are in hcp sites in the small region in between the brighter lines. (c) A schematic sketch of the stacking fault region. Regions of fcc stacked Co are separated from smaller areas of hcp Co by partial dislocations, in which the Co atom occupies mostly bridge sites explaining the brighter appearance of the dislocation lines.

which it is shown that the atoms in between the brighter lines occupy hcp sites. A schematic model of a partial dislocation is shown in Fig. 3(c). From Figs. 2(b) and 3 it is clear that Co takes preferably the Pt fcc lattice sites, with a smaller number of Co atoms in disordered (bridge) or in hcp sites due to the stress in the Co overlayer.

Due to the mismatch of -9.4% between the Co [nearest-neighbor (nn) distance 2.51 Å) and the Pt (nn 2.77 Å) lattice, the Co overlayer becomes strained, which is relieved by the partial dislocations (tensile strain). Similar dislocation lines have in the recent past been observed for a number of clean surfaces and thin metal film on metal substrate systems.[18–21] Such a dislocation system may be described by the Frenkel-Kontorova model[22] for a weakly incommensurate phase. This model is characterized by two competing interactions, the interatomic in-plane interaction between the Co atoms and a corrugated substrate potential. In the present case, the system obviously achieves the lowest energy by occupying most of the substrate's corrugation minima (hollow sites), and squeezing a few atoms close together, creating a heavy domain wall (partial dislocations). The domain wall is observed as brighter appearing Co atoms on the border between the fcc and the hcp regions since these atoms occupy mainly bridge positions. The close distance between the two domain walls adjacent to the hcp area in Fig. 2(b) is due to the preference of the Co layer to grow in an fcc as compared to hcp stacking, resulting in only small hcp regions in the first layer. It would be expected that the small difference in stacking fault energy for Co would lead to approximately equal areas of hcp and fcc regions, which is not observed. The reason for the observed large differences in

fcc and hcp areas may be due instead to a proximity to a commensurate phase.[23]

In addition, brighter single atoms may also be observed in the Co layer. These atoms are Pt atoms, which may be realized by comparing the similar appearance of these atoms with the Pt atoms at the Pt step edge [lower right in Fig. 2(b)], indicating a very limited diffusion of Pt atoms to the surface.

The formation of the second Co layer on top of the first layer results in the formation of a moiré structure as shown in Fig. 2(c). This structure is a result of a different in-plane lattice spacing of the Co overlayer as compared to that of the Pt lattice in the Pt(111) surface, and has been observed previously with STM in this system[8] as well as for other systems, e.g., Ref. 24. From the periodicity of the moiré structure it is possible to deduce the contraction of the in-plane lattice spacing as compared to the in-plane lattice spacing in the Pt(111) surface from the moiré formula.[26] An STM image from 2.5 ML of Co on Pt(111) is shown in Fig. 4(a). We find that the periodicity of the moiré structure is 12.7 ± 1.1 Co atoms resulting in a Co in-plane lattice constant contracted by $7.9 \pm 0.7\%$ as compared to the Pt (111) in-plane lattice distance, slightly more than 6% as found in the previous STM study.[8] The corresponding number for bulk Co is 9.4%. A hard-sphere model for the Pt-Co interface showing the moiré structure is shown in Fig. 4(c).

As we increase the Co coverage on the Pt(111) surface, the Co-induced moiré structure persists, as shown by a set of 100×100 nm^2 STM images in Fig. 5. Figure 5(a) shows an STM image of 2.2 ML of Co deposited at the Pt(111) surface at RT. In this image, at least three levels displaying a moiré structure may be observed. The large, flat areas from which the moiré structure may be observed indicate that the ordering in the second Co layer is higher than the observed ordering in the first Co layer in Fig. 2(b). Therefore, we conclude that the dislocations observed in the first Co layer [see Fig. 2(b)] are lifted as the second Co layer is being formed. The above observation is in agreement with the conclusions drawn from the previous STM study.[8] Further, in the case of epitaxial films of Cu and Ni on Ru(0001) with a 5.5% and 8.1% lattice distance mismatch, respectively (tensile strain),[19,20] rearrangements of several layers have been observed as additional layers are deposited. Also, recent studies of thin films of Ag on Pt(111) (Ref. 27) have shown that partial dislocations observed (in this case due to 4.3% compressive strain) in the first Ag layer may be relieved by the second Ag layer. For the present system, it should be noted, since STM is only sensitive to the topmost layer, a possible small diffusion of Pt into the first Co layer during the rearrangement of this layer cannot be excluded.

Figure 5(b) shows an STM image of an approximately 3.5 ML thick Co film on the Pt(111) surface. In this case, five levels displaying the moiré structure may be observed. The steps of the adislands have become more straight (the number of kinks and corners have been reduced), i.e., the step coarsening has decreased. The reduced number of kinks and corners should lead to a higher effective Schwoebel barrier.[25] An STM image from 5 ML of Co is shown in Fig. 5(c). At least six levels displaying a moiré structure may be observed. The step coarsening has decreased further, and the size of the adislands has increased. Also, some islands have a more triangular shape. The corrugation of the moiré structure is decreasing as the coverage is increasing, reflecting the number of levels between the observed terraces, and the interface between the Pt(111) surface and the first Co-layer (causing the moiré structure).

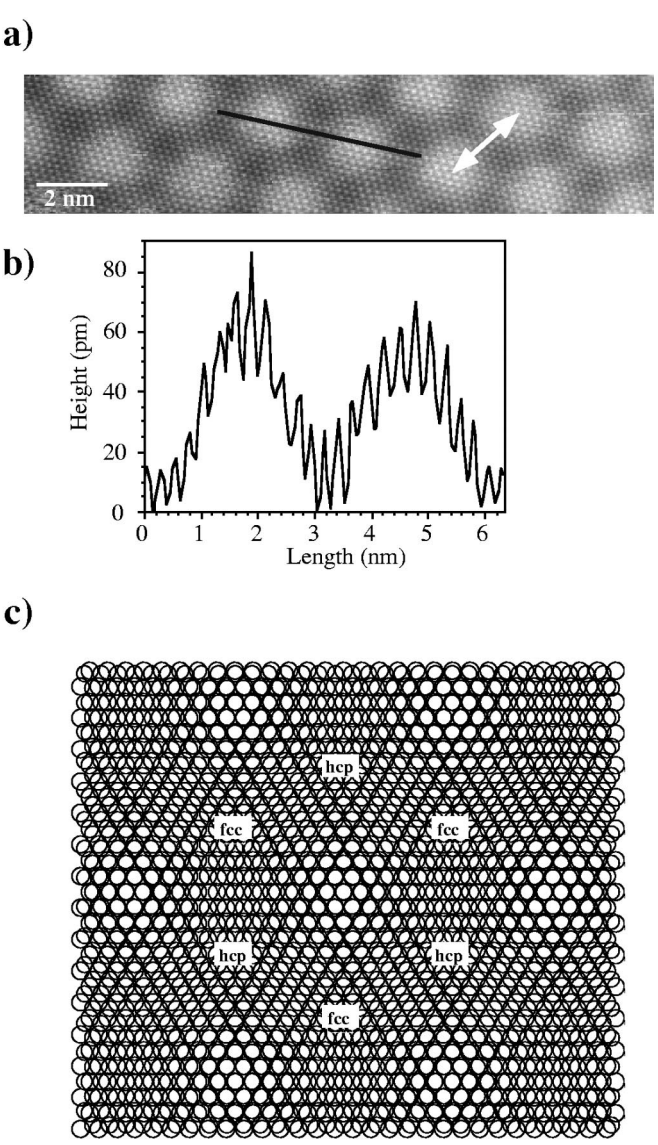

FIG. 4. (a) STM image with atomic resolution of a 2.5 ML thick Co film deposited on the Pt(111). The white arrow indicates the periodicity of 12.7 ± 1.1 Co atoms of the moiré structure. (b) Line scan showing the corrugation of the Co film corresponding to the black line in Fig. 4(a). (c) Top view of a hard-sphere model of the atomic arrangement of the Pt(111) substrate and the first 7.9% contracted Co layer, resulting in the moiré structure.

By comparing the periodicity of the moiré structure in STM images recorded from samples with different Co coverages, we observe no change as the Co coverage is increased, indicating no additional change of the in-plane lattice constant of the Co overlayer within our detection limits. It should also be noted that we cannot determine whether Co grows in an fcc or an hcp stacking sequence based on the lattice constant as obtained from the moiré structure, since the in-plane lattice distances for Co(111) and Co (0001) are very similar.

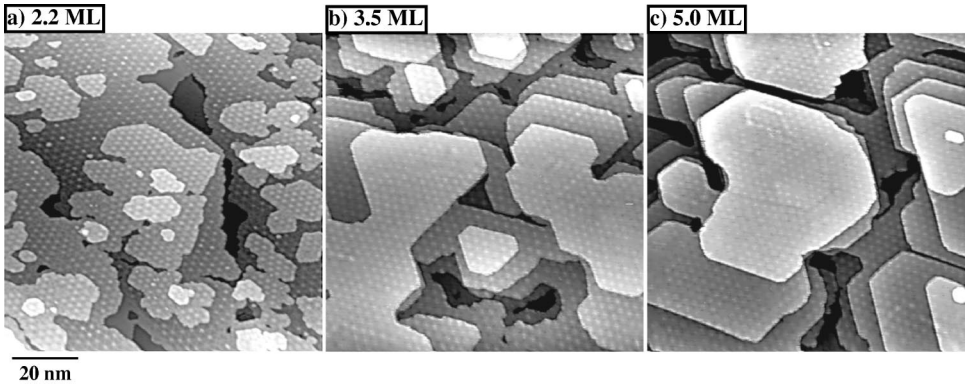

FIG. 5. STM images showing the development of the moiré structure and the surface morphology displayed by the Co thin film with increasing Co coverages for (a) 2.2 ML of Co, (b) 3.5 ML, and (c) 5 ML of Co.

B. High Co coverages on the Pt(111) surface (3.5–15 ML)

Figure 6 shows a set of 300×300 nm^2 STM images with Co coverages ranging from 3.5 to 15 ML deposited on Pt(111) at RT. As the influence of the moiré structure is reduced with higher Co coverage (5 ML and higher), we observe pyramidal islands with triangular shape. The triangular shape is due to the existence of two types of steps on a (111) surface, the so-called *A* and *B* steps, with (111) and (100) microfacets, respectively. If one facet is preferred energetically or has a different growth speed (the detailed process is irrelevant in the present context), instead of hexagons (sixfold symmetry) we will observe triangles (threefold symmetry). Further, if the same microfacet is favored independent of the Co thickness, and if the step-step distance is large enough to allow any direction of the step, fcc stacking and hcp stacking will lead to triangles stacked facing the same or the opposite direction, respectively. Examples of these two cases are indicated in Fig. 6(b). Thus, we may conclude that in the top layers both fcc and hcp stacking are present at a Co coverage of 5 ML, however with clear predominance of fcc stacking. For the lower levels, we cannot determine the stacking sequence in this way, as the distance between the steps is too small to allow for alternating orientation of triangular terraces. The shape of the terraces in these levels is rather dominated by the repulsive step-step interaction.

Even though the above arguments are convincing and have been used in previous STM investigations,[8] the fact that Co is observed to grow in an fcc stacking sequence is surprising. Therefore, we show an additional proof for this conclusion in Fig. 7, in which we analyze a defect observed on an island such as shown in Fig. 7(a) from a Co film with a thickness of 8 ML. There, a straight step with a height of $\frac{1}{3}$ of the height of a normal Co step is found on the upper terrace. In continuation of this $\frac{1}{3}$ step, on the lower terraces there are steps with $\frac{2}{3}$ height, but facing the opposite direction (i.e., step-down when moving from upper left to lower

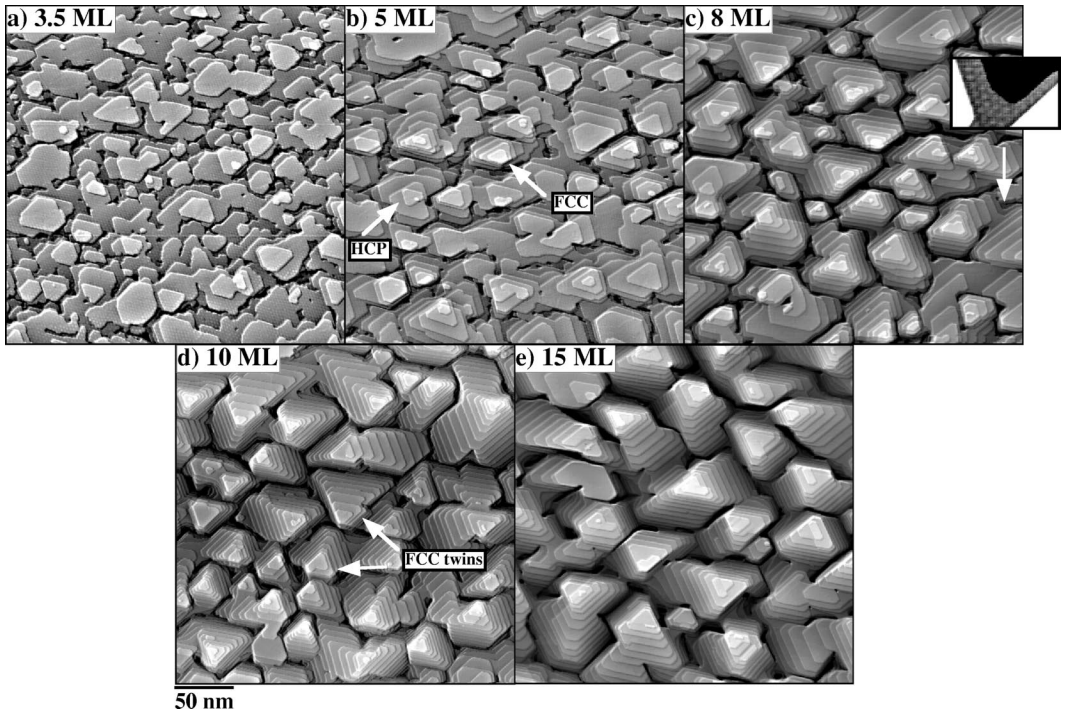

FIG. 6. STM images showing the development of the growth and morphology of thin Co films on Pt(111). (a) STM image of a 3.5 ML thick Co film. (b) STM image of a 5 ML thick Co film. The arrows indicates islands with fcc and hcp Co stacking. (c) STM image of an 8 ML thick Co film. The inset shows an STM image demonstrating the moiré structure observable in the valleys between the islands. (d) STM image of a 10 ML thick Co film. The arrows indicates the existence of fcc twins. (e) STM image of a 15 ML thick Co film.

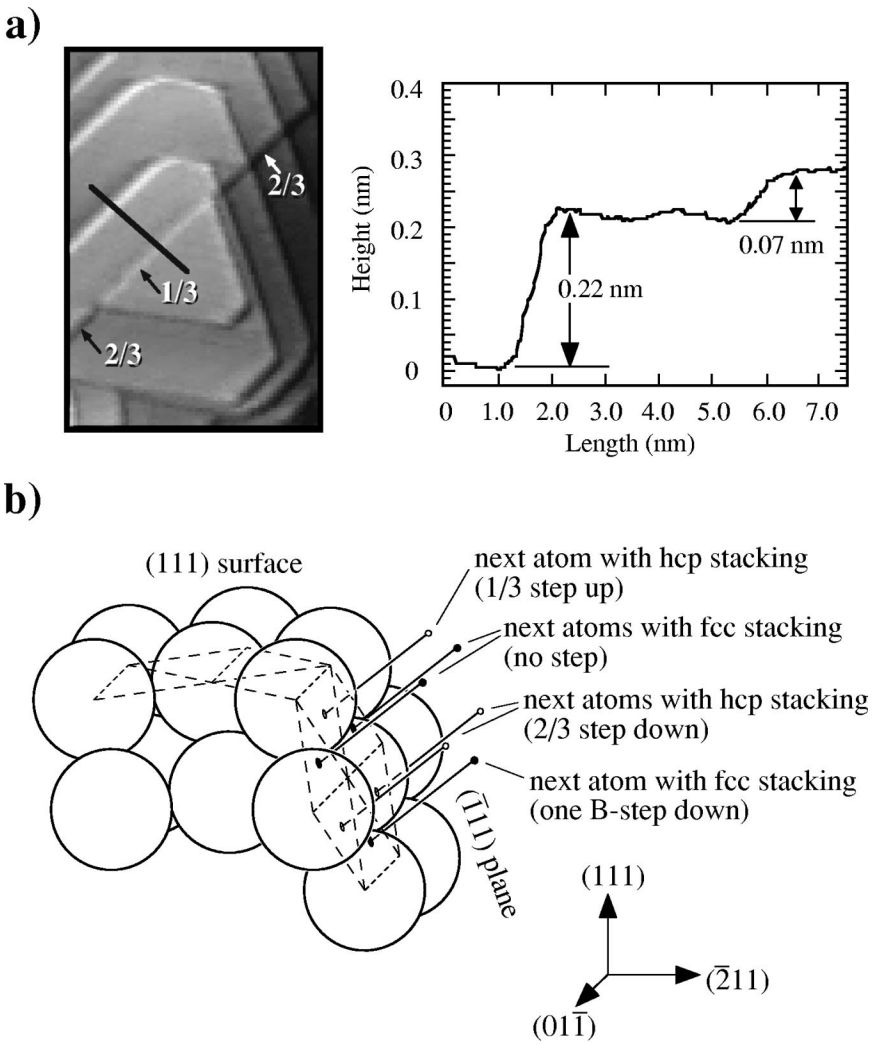

FIG. 7. (a) STM image of an 8 ML thick Co film on Pt(111) showing a stacking fault in a Co island. The line scan across a step and the intersection of the stacking fault plane with the surface demonstrates that the height of the Co step is approximately 0.22 nm while the stacking fault results in a step height of 0.07 nm or $\frac{1}{3}$ of the Co step height on the upper terrace. On the lower terraces, $\frac{2}{3}$ steps are found. Fractions $\frac{1}{3}$ and $\frac{2}{3}$ in the image give the step height as a multiple of the interlayer distance of fcc Co(111). (b) The model shows how a stacking fault in a $(\bar{1}11)$ plane is formed. Black dots show the positions of the atoms' centers without a stacking fault (fcc lattice), whereas the open dots give the position of atoms in the hcp hollow sites of the $(\bar{1}11)$ plane. This allows us to conclude that $\frac{2}{3}$ steps caused by the intersection of a stacking fault with the surface have the same orientation as B steps on a regular fcc lattice, whereas $\frac{1}{3}$ steps caused by a stacking fault have the orientation of *A* steps.

right in the image). This is a clear fingerprint of a stacking fault plane intersecting an fcc (111) surface. The model [Fig. 7(b)] shows how such a stacking fault is formed by placing atoms into the hcp sites of a $(\bar{1}11)$ plane. Such a stacking fault may *only* exist in an fcc stacked film.[28] These stacking faults are commonly observed in the islands. At least seven of the islands in Fig. 6(e) exhibit such stacking faults. No dislocations typical for hcp stacking have been found on any of the islands identified as fcc via the shape of the terraces. On the other hand, the islands identified as hcp [see Fig. 6(b)] never show stacking faults as the one shown in Fig. 7. Since most islands without a stacking fault show the same island shape at the top as those with an fcc stacking fault, we must therefore conclude that the stacking sequence is fcc almost everywhere for Co coverages of 5 ML and above. If the triangles are alternating, we have to conclude that they are stacked in an hcp sequence, as indicated in Fig. 6(b). Further, as stated above, it is clear that one of the step orientations is favored. The stacking fault shown in Fig. 7 provides us with the relevant information in order to determine which. It is obvious from Fig. 7(b) that the orientation of a $\frac{2}{3}$ step caused by a stacking fault is the same as that of a *B* step (descending when crossing it in the $[\bar{2}11]$ direction). A $\frac{1}{3}$ step has the opposite direction (ascending when crossing it in the $[\bar{2}11]$ direction) and therefore the same orientation as an *A* step. Thus we find that the longer sides of the triangles are *A* steps, as opposed to the predominant facet present during growth of Pt on Pt(111) at intermediate temperatures, which was found to be a *B* step.[25] In addition, since the stacking fault is observed to run all the way to the bottom of the island, it is clear that the geometry of the islands does not change as the triangles are stacked on top of each other.

Returning to Fig. 6(a), which corresponds to a Co coverage of 3.5 ML, hardly any characteristic island shapes re-

flecting the stacking sequence of the Co layers are observed, even though the Co coverage is sufficient to speak of hcp or fcc stacking. Thus we are not able to distinguish between fcc and hcp Co in the coverage region between 1 and 3.5 ML, neither from the moiré structure nor from the shape of the islands. Many steps are rather irregular, quite in contrast to the straight steps found at higher coverages. It is well known that dislocations may disturb and influence island nucleation.[29] The moiré structure as discussed above is direct evidence for an undulating surface with a resulting variation of the in-plane and out-of-plane lattice distances, which is likely to influence the preference of the growth directions of the islands.

In Fig. 6(c), corresponding to 8 ML of Co, triangular shaped islands with more than 10 levels may be observed. It is clear from Fig. 6(c) that the vast majority of these triangles does not change orientation from layer to layer, directly demonstrating that Co grows in a predominantly fcc structure at this Co coverage. In fact, the images presented in Figs. 6(c)–6(e) are very similar to recent STM images presented for Pt on Pt(111),[25] which grows with an fcc stacking sequence. The moiré structure induced by the Co is visible at the lower levels in the valleys between the islands, as illustrated by the inset in Fig. 6(c). Further, two opposite directions of the triangles may be identified as indicated in Fig. 6(d), demonstrating the existence of fcc twins, the stacking sequence being $ABC\ldots$ and $CBA\ldots$, due to stacking faults in a lower level. It should be noted that the existence of the twins, if the domains of the twins have an approximately equal area as in the present case, will cause the observed superstructure spots due to the Co in-plane lattice in LEED to have a sixfold symmetry. Finally, in Fig. 6(e) is shown an STM image from 15 ML of Co. The appearance of the islands is similar in Figs. 6(c) and 6(d), the difference being that the island sizes become larger as the Co coverage is increased.

The present study for Co coverages of above 5 ML directly demonstrates that Co grows with a predominantly fcc stacking sequence. This result is in agreement with previous x-ray studies,[14,15] but in disagreement with the observations made in the earlier STM study[8] and EXAFS measurements.[10] These contradictory results concerning the stacking sequence of Co may be compared to those that have been obtained for Co/Cu(111), further illustrating the difficulties that exist in determining the stacking sequence of thin Co films. X-ray-diffraction measurements[30] of 4 nm thick multilayers of Co and Cu on Cu(111) concluded that Co grows in a predominantly twinned fcc stacking sequence. For a single Co film on Cu(111) the results reported in the literature for Co films up to a thickness of 5.5 ML vary depending on the number of steps on the surface or segregation of Cu to the surface of the Co film.[31–33] Above 5.5 ML, indirect investigations based on the magnetic properties indicated Co films stacked in a fcc sequence,[34] but no clear distinction between hcp and fcc could be made.

As a quantitative criterion allowing to distinguish between 2D and 3D growth of the Co films, Fig. 8 shows the fraction of the terrace levels as estimated from the STM images in Figs. 5(a) and 6(a)–6(e). In the case of pure 2D growth, interlayer diffusion across step edges to a lower terrace must be present, resulting in a limited number of levels.

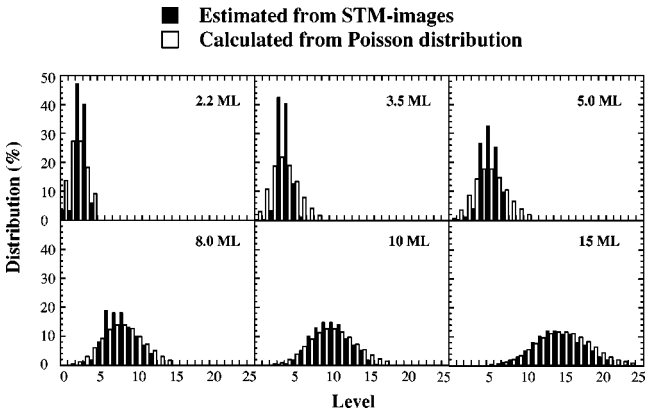

FIG. 8. Estimation of the distribution of the fraction of levels present in the STM images shown in Fig. 5(a) and Figs. 6(a)–6(e), and the fraction calculated from a Poisson distribution for each coverage as would be expected for a 3D growth with no interlayer diffusion (Ref. 35). Note the improved agreement between the experimental and calculated values as the Co coverage is increased. The Co coverage is indicated in each plot.

In the case of pure 3D growth, in which no interlayer diffusion is present, the distribution of the terrace levels is expected to follow a Poisson distribution.[35] Therefore, the expected Poisson distribution of the number of levels for each Co coverage is also plotted in Fig. 8. It may be seen from this figure that the data points agree fairly well with the Poisson distribution at higher Co coverages, but at lower coverages two terrace levels make up most of the image area, adding support for a 2D growth mode in this coverage region. It should be noted that the estimation of the level distribution from the STM images is not straightforward, due to difficulties in observing underlying steps, completely filled levels (the ''0'' level is unknown for higher coverages), and the limited sharpness of the STM tip. We believe that the resulting errors are sufficiently small, however, to allow a clean discrimination between 2D and 3D growth.

IV. DISCUSSION

We suggest that the reason for the 2D growth mode at lower Co coverages is due to rough step edges caused by the highly strained interface between the Co and the Pt(111) surface. The strained interface results in the moiré structure which in turn results in an overlayer with a high density of kinks and corners. Such sites are common in the present system in the Co films with 1–5 ML of Co. The presence of such an overlayer is likely to facilitate 2D growth since it is known[25,36–39] that sites such as kinks and corners are favorable sites for adatom interlayer diffusion. As the coverage is increased, the influence of the strained interface decreases, resulting in a lower number of kinks and corners (reduced step-coarsening), which in turn results in a 3D growth. It should, however, be noted that the diffusivity of adatoms may change as the influence of the strained interface is decreasing, i.e., as the thickness of the added film is increased,[20,29] which may additionally affect the morphology of the Co film.

Finally, we would like to comment on previous findings concerning the relation between changes observed in the PMA and the structure of the Co film. In Ref. 7, PMA was

observed up to a Co coverage of approximately 4–6 ML, while at higher Co coverages it disappeared and instead in-plane anisotropy was observed. In light of previous findings from thin Pt/Co/Pt sandwiches,[5,6] a possible relationship between the change of the magnetic properties at the interface and the structure would be a change in the stacking from fcc to hcp with increasing Co coverage. However, in the present investigation, we do not find any evidence for such a behavior; instead we find, in this coverage regime, a change from a 2D growth mode to a 3D growth mode.

Since the interface is expected to give a contribution to the magnetic anisotropy,[40] the decrease of the PMA coinciding with the appearance of a 3D growth mode may explain the SMOKE results. We speculate that the onset of the 3D growth as observed in the present investigation may thus result in a reduced importance of the influence from the interface on the observed magnetic anisotropy, i.e., the volume anisotropy overcomes the Co/Pt interface anisotropy, confirming conclusions based on LEED and AES in Ref. 12. Such a scenario is also consistent with the known importance of the ''sharpness'' of the interface.[41]

Further, a parameter which has been observed to influence the PMA is a change in the lattice constant in the out-of-plane direction.[42] In the present system, such a change *is* present in the Co layers with increasing Co coverage, since the moiré structure exhibits a modulated out-of-plane lattice distance at low Co coverages, which become less pronounced with increasing Co coverage as the Co relaxes to its bulk lattice constant. Thus, this change may be of importance since it also coincides with the observed change in the PMA. Using STM to determine vertical displacements as such which are under consideration for the present system is not appropriate, due to the uncertainties involved in such measurements. Further, reliable details of the structure on the atomic level, which would be needed as an input for theoretical investigations to study the influence of vertical strain on magnetic properties, are unfortunately difficult to obtain for the present system using a diffraction technique such as LEED due to the large unit cell of the moiré structure. A more suited technique for such a determination would be SXRD due to the kinematical nature of x-ray diffraction.

V. SUMMARY

In summary, we have studied the evolution of the structure, growth, and morphology of thin Co films deposited at RT on Pt(111) using STM. We have demonstrated that the first Co layer resides predominantly in the Pt fcc hollow sites. The strain in the Co layer is relieved by the formation of dislocations resulting in smaller areas of Co in hcp sites, the fcc and hcp areas being separated by Co in bridge sites. The second Co layer is found to relieve the strain in the first layer, resulting in the formation of a hexagonal moiré structure, the Co in-plane lattice distance being close to that of bulk Co. The moiré structure persists up to a Co coverage of at least 5 ML. The growth appears to be smooth or 2D up to a Co coverage of about 3.5 ML. Above this coverage a 3D growth is observed. The Co layers in these triangular shaped islands are shown to be stacked in a predominantly twinned fcc stacking.

ACKNOWLEDGMENT

This work was supported by the Fonds zur Förderung der wissenschaftlichen Forschung (START-program Y75) and the TMR program Marie Curie Research Training Grants of the European Union. We gratefully acknowledge Professor P. Weinberger for stimulating discussions.

[1] See, for example, H. Brune, Surf. Sci. Rep. **31**, 1998 and references therein.
[2] P. F. Carcia, A. D. Meinhaldt, and A. Suna, Appl. Phys. Lett. **47**, 178 (1985).
[3] W. B. Zeper, F. J. A. M. Greidanus, P. F. Garcia, and C. R. Fincher, J. Appl. Phys. **65**, 4971 (1989).
[4] N. W. E. McGee, M. T. Johnsson, J. J. de Vries, and J. aan de Stegge, J. Appl. Phys. **73**, 3418 (1993).
[5] N. Nakajima, T. Koide, T. Shidara, H. Miauchi, H. Fukutani, A. Fujimori, K. Iio, T. Katayama, M. Nyvlt, and Y. Suzuki, Phys. Rev. Lett. **81**, 5229 (1998).
[6] D. Weller, A. Carl, R. Savoy, T. C. Huang, M. F. Toney, and C. Chappert, J. Phys. Chem. Solids **56**, 1563 (1995).
[7] C. S. Shern, J. S. Tsay, H. Y. Her, Y. E. Wu, and R. H. Chen, Surf. Sci. **429**, L497 (1999).
[8] P. Grütter and U. T. Dürig, Phys. Rev. B **49**, 2021 (1994); J. Vac. Sci. Technol. B **12**, 1768 (1994).
[9] P. Grütter and U. T. Dürig, Surf. Sci. **337**, 147 (1994).
[10] J. Thiele, R. Belkhou, H. Bulou, O. Heckman, H. Magnan, P. Le Févre, D. Chanderis, and C. Guillot, Surf. Sci. **120**, 384 (1997).
[11] J. Thiele, N. T. Barrett, R. Belkhout, C. Guillot, and H. Koundi, J. Phys.: Condens. Matter **6**, 5025 (1994).
[12] J. S. Tsay and C. S. Shern, Surf. Sci. **396**, 313 (1998); **396**, 319 (1998).
[13] M. Henzler, Surf. Sci. **419**, 321 (1999).
[14] S. Ferrer, J. Alvarez, E. Lundgren, X. Torrelles, P. Fajardo, and F. Boscherini, Phys. Rev. B **56**, 9848 (1997).
[15] M. C. Saint-Lager, R. Baudoing-Savois, M. De Santis, P. Dolle, and Y. Gauthier, Surf. Sci. **418**, 485 (1998).
[16] C. Nagl, O. Haller, E. Platzgummer, M. Schmid, and P. Varga, Surf. Sci. **321**, 237 (1994).
[17] E. Lundgren, B. Stanka, W. Koprolin, M. Schmid, and P. Varga, Surf. Sci. **423**, 357 (1999).
[18] M. Bott, M. Hohage, T. Michely, and G. Comsa, Phys. Rev. Lett. **70**, 1489 (1993).
[19] C. Günter, J. Vrijmoeth, R. Q. Hwang, and R. J. Behm, Phys. Rev. Lett. **74**, 754 (1995).
[20] J. A. Meyer, P. Schmid, and R. J. Behm, Phys. Rev. Lett. **74**, 3864 (1995).
[21] J. de la Figuera, K. Pohl, A. K. Schmid, N. C. Bartel, J. Hrbek, and R. Q. Hwang, Surf. Sci. **433-435**, 93 (1999).
[22] J. Frenkel and T. Kontorova, Zh. Eksp. Teor. Fiz. **8**, 1340 (1939).
[23] J. C. Hamilton, R. Stumpf, K. Bromann, M. Giovannini, K. Kern, and H. Brune, Phys. Rev. Lett. **82**, 4488 (1999).
[24] T. A. Land, T. Michely, R. J. Behm, J. C. Hemminger, and G. Comsa, Surf. Sci. **264**, 261 (1992).
[25] M. Kalff, P. Smilauer, G. Comsa, and Th. Michely, Surf. Sci. **426**, 3 (1999).

[26] B. A. Parkinson, F. S. Ohuchi, K. Ueno, and A. Koma, Appl. Phys. Lett. **58**, 272 (1991).
[27] K. Bromann, H. Brune, M. Giovannini, and K. Kern, Surf. Sci. **388**, 1107 (1997).
[28] J. P. Hirth and J. Lothe, *Theory of Dislocations*, 2nd ed. (Wiley, New York, 1982).
[29] H. Brune, K. Bromann, H. Röder, K. Kern, J. Jacobsen, P. Stoltze, K. Jacobsen, and J. Nörskov, Phys. Rev. B **52**, 14 380 (1995).
[30] F. J. Lamelas, C. H. Lee, Hui He, W. Vavra, and Roy Clarke, Phys. Rev. B **40**, 5837 (1989).
[31] J. de la Figuera, J. E. Prieto, C. Ocal, and R. Miranda, Phys. Rev. B **47**, 13 043 (1993).
[32] S. Müller, G. Kostka, T. Schäfer, J. de la Figuera, J. E. Prieto, C. Ocal, R. Miranda, and K. Heinz, Surf. Sci. **352-354**, 46 (1994).
[33] Ch. Rath, J. E. Prieto, S. Müller, G. Kostka, R. Miranda, and K. Heinz, Phys. Rev. B **55**, 10 791 (1997).
[34] M. Farle, W. Platow, E. Kosubek, and K. Baberschke, Surf. Sci. **317**, 146 (1999).
[35] K. Meinel, M. Klaua, and H. Bethge, J. Cryst. Growth **89**, 447 (1989).
[36] M. Villarba and H. Jonsson, Surf. Sci. **317**, 15 (1994).
[37] J. Jacobsen, K. W. Jacobsen, P. Stoltze, and J. K. Nørskov, Phys. Rev. Lett. **74**, 2295 (1995).
[38] E. Lundgren, B. Stanka, G. Leonardelli, M. Schmid, and P. Varga, Phys. Rev. Lett. **82**, 5068 (1999).
[39] G. Leonardelli, B. Stanka, E. Lundgren, M. Schmid, and P. Varga (unpublished).
[40] L. Neel, J. Phys. Radium **15**, 225 (1954).
[41] F. J. A. den Broeder, D. Kuiper, A. P van de Mosselaer, and W. Howing, Phys. Rev. Lett. **60**, 2769 (1988).
[42] C. Uiberacker, J. Zabloudil, P. Weinberger, L. Szunyogh, and C. Sommers, Phys. Rev. Lett. **82**, 1289 (1999).